VIP In-Cell NMR Spectroscopy Very Important Paper

International Edition: DOI: 10.1002/anie.201500261
German Edition: DOI: 10.1002/ange.201500261

# Direct Observation of $Ca^{2+}$-Induced Calmodulin Conformational Transitions in Intact *Xenopus laevis* Oocytes by $^{19}F$ NMR Spectroscopy**

*Yansheng Ye, Xiaoli Liu, Guohua Xu, Maili Liu, and Conggang Li**

***Abstract:*** *The $Ca^{2+}$-mediated conformational transition of the protein calmodulin (CaM) is essential to a variety of signal transduction pathways. Whether the transition in living cells is similar to that observed in buffer is not known. Here, we report the direct observation by $^{19}F$ NMR spectroscopy of the transition of the $Ca^{2+}$-free and -bound forms in Xenopus laevis oocytes at different $Ca^{2+}$ levels. We find that the $Ca^{2+}$-bound CaM population increased greatly upon binding the target protein myosin light-chain kinase (MLCK) at the same $Ca^{2+}$ level. Paramagnetic NMR spectroscopy was also exploited for the first time to obtain long-range structural constraints in cells. Our study shows that $^{19}F$ NMR spectroscopy can be used to obtain long-range structural constraints in living eukaryotic cells and paves the way for quantification of protein binding constants.*

Calmodulin (CaM), an intracellular $Ca^{2+}$ sensor protein with two $Ca^{2+}$ binding domains, is involved in many $Ca^{2+}$-mediated signaling pathways. In smooth muscle, $Ca^{2+}$ binds CaM, thereby inducing a conformational change that enables binding to myosin light-chain kinase (MLCK). This binding activates the kinase, which is key to muscle contraction.[1] Studies in buffer show that $Ca^{2+}$-bound CaM (Ca-CaM) binds various cellular targets with dissociation constants ($K_d$) ranging from nM to μM (Figure 1).[2] CaM signaling may be regulated by these different affinities, but whether the conformational transitions, binding affinities, and structures in cells are similar to those in buffer is not known, because direct experimental verification in living cells is challenging.

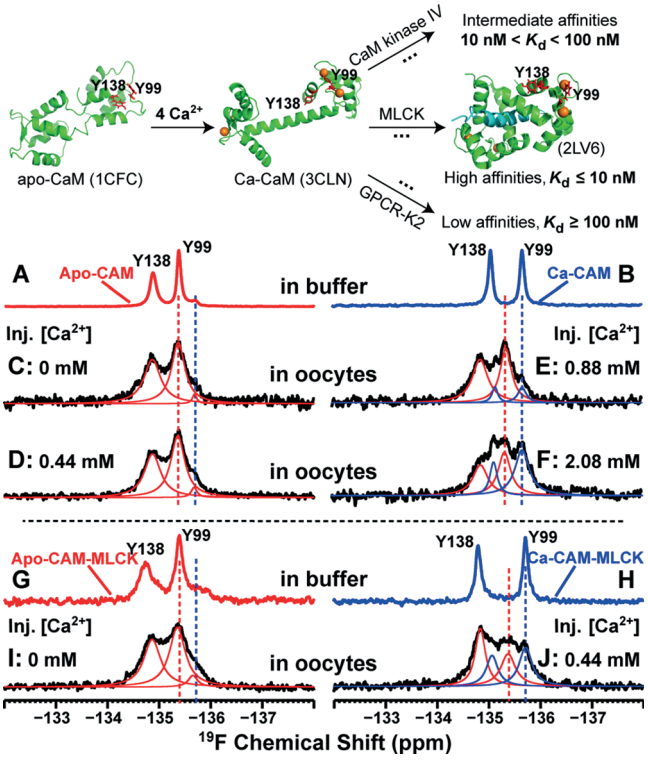


***Figure 1.*** Conformational transitions of CaM in the presence of $Ca^{2+}$ and cellular targets with different $Ca^{2+}$ affinities (PDB_ID: 1CFC for apo-CaM, 3CLN for Ca-CaM, and 2LV6 for the CaM MLCK complex). The location of the $^{19}F$ labels at Y99 and Y138 are shown. One-dimensional $^{19}F$ NMR spectra of 3FY-labeled $Ca^{2+}$-free (apo-CaM, red; A) and $Ca^{2+}$-bound (Ca-CaM, blue; B) in buffer and in *Xenopus* oocytes injected with ≈20 nL of 5 mM apo-CaM in the presence of 0 (C), 22 (D), 44 (E), and 104 (F) mM $Ca^{2+}$ per oocyte. The injected final intracellular $Ca^{2+}$ concentrations are estimated to be 0, 0.44, 0.88, and 2.08 mM, as indicated. One-dimensional spectra of 3FY-labeled $Ca^{2+}$-free (apo-) CaM-MLCK (red) in buffer (G) and in oocytes (I), and $Ca^{2+}$-bound (Ca-) CaM-MLCK in buffer (H) and in oocytes (J). The red and blue dashed lines indicate chemical shifts from the buffer data. The peaks in the oocyte spectra were fitted according to the buffer data for apo-Cam, Ca-CaM, or CaM-MLCK.

In-cell NMR spectroscopy can monitor protein conformational transitions in living cells at atomic resolution.[3] For example, $^{15}N$-$^{1}H$ HSQC spectra have been used to study the maturation of superoxide dismutase in live human cells.[3b] Nevertheless, it is known that most globular proteins yield low-quality (or even undetectable) in-cell $^{15}N$-$^{1}H$ HSQC spectra because the high cellular viscosity and ubiquitous weak interactions in cells (compared to buffer) lead to broad

[*] Y. Ye, X. Liu, Dr. G. Xu, Prof. Dr. M. Liu, Prof. Dr. C. Li
Key Laboratory of Magnetic Resonance in Biological Systems
State Key Laboratory of Magnetic Resonance and Atomic and Molecular Physics, National Center for Magnetic Resonance in Wuhan, Wuhan Institute of Physics and Mathematics
Chinese Academy of Sciences
Wuhan 430071 (China)
E-mail: conggangli@wipm.ac.cn
Y. Ye
Graduate University of Chinese Academy of Sciences
Beijing 100049 (China)

[**] This work was supported by the Ministry of Science and Technology of China (grant 2013CB910200), the 1000 Young Talents Program, and National Natural Sciences Foundation of China (grants 21173258, 21120102038, and 21221064).

Supporting information for this article (sample preparation, NMR experimental details, $^{15}N$-$^{1}H$ HSQC spectra, and $^{19}F$ NMR spectra) is available on the WWW under http://dx.doi.org/10.1002/anie.201500261.

signals.[4] The $^{15}N$-$^{1}H$ HSQC spectrum of CaM in *Xenopus* oocytes displays broad, unresolved cross-peaks, which makes it impossible to distinguish conformational states (see Figure S1 in the Supporting Information). $^{19}F$ NMR spectroscopy has been used to show that CaM in *Escherichia coli* mainly exists in the $Ca^{2+}$-free apo form.[5] We turned to *Xenopus laevis* oocytes, a model eukaryotic cell system, to study the CaM conformational transition and CaM function because the $Ca^{2+}$ level is difficult to manipulate in *E. coli* and because CaM is native to eukaryotes.

To monitor the conformational transition at different $Ca^{2+}$ concentrations in oocytes, Y99 and Y138 were replaced with 3-fluorotyrosine (3FY). As shown in Figure 1 A,B, the $^{19}F$ NMR spectra of the $Ca^{2+}$-free (apo-CaM) and $Ca^{2+}$-bound (Ca-CaM) forms show distinct shifts in buffer, consistent with previous reports.[6] Resonance assignments were made by site-directed mutagenesis (see Figure S2 in the Supporting Information). We then injected approximately 20 nL of 5 mM apo-CaM along with increasing amounts of $Ca^{2+}$. The range of $Ca^{2+}$ concentrations is 0 to 2 mM, assuming an oocyte volume of 1 μL. Spectra were then recorded as a function of the $Ca^{2+}$ concentration (Figure 1 C–F). The resonances in cells are broader than those in dilute solution. The conformational state of CaM in cells was inferred by comparing the in-cell spectrum to that obtained in buffer. The in-cell signals were deconvoluted using the buffer data to yield the populations of apo- (red) and Ca-CaM (blue).

When apo-CaM was injected, the $^{19}F$ NMR spectrum (Figure 1 C) of the apo form is observed in cells, which suggests that the concentration of free $Ca^{2+}$ is very low in oocytes, consistent with reports.[4a] The level of the apo form did not change over the course of 12 h. However, the Ca-bound form was observed after 18 h (see Figure S3 in the Supporting Information), which may be due to $Ca^{2+}$ bursts from cell stress induced after such a long time in the NMR tube, as reported for HeLa cells.[3d]

To our surprise, when $Ca^{2+}$-bound CaM (final intracellular $Ca^{2+}$ concentration 0.44 mM) was injected, the $^{19}F$ NMR spectrum (Figure 1 D) showed only the apo form, thus suggesting that $Ca^{2+}$ was stripped from the protein after injection. We speculate that the $Ca^{2+}$ loss may be due to competitive binding of some cell components. To address this possibility, we conducted competitive binding experiments in buffer between Ca-CaM and $Mg^{2+}$ (the most abundant divalent cation in cells), membrane components, nucleic acids from *E. coli* and oocyte extracts (see Figure S4 in the Supporting Information). None of these conditions transformed Ca-CaM into apo-CaM. This result further indicates that $Ca^{2+}$ is strictly regulated in living cells, possibly by $Ca^{2+}$ pumps and exchangers.[7] We then increased the injected final intracellular $Ca^{2+}$ concentration to 0.88 mM. The resulting spectrum (Figure 1 E) indicated the presence of Ca-CaM, with the peak fitting indicating a molar ratio of apo-CaM to Ca-CaM of approximately 6:1. When the injected intracellular $Ca^{2+}$ concentration was increased to 2 mM, the spectrum (Figure 1 F) showed an increased population of Ca-CaM (molar ratio of apo-CaM to Ca-CaM of $\approx$ 1:1). These observations suggest that the protein can be saturated at high intracellular $Ca^{2+}$ concentrations.

To test ideas about target activation, we injected the CaM-MLCK complex in the absence and presence of $Ca^{2+}$ (Figure 1 I,J). The complex was constructed as described.[8] Briefly, 26 residues from the MLCK binding peptide were inserted into the C-terminus of CaM. This construct has a similar response to $Ca^{2+}$ as CaM with an unattached MLCK peptide.[8] Figure 1 G–J shows the $^{19}F$ NMR spectra of apo- and Ca-CaM-MLCK in buffer and oocytes. Similar to what we observed for CaM, the chemical shift is sensitive to the apo and Ca form of the complex in buffer. Injected apo-CaM-MLCK remains in the apo form after injection (Figure 1 I). In contrast to what we observe with injected CaM (Figure 1 D), both apo- and Ca-CaM-MLCK are present at a final intracellular injected $Ca^{2+}$ concentration of 0.44 mM (Figure 1 J, ca. 1:1 molar ratio of apo- to Ca-CaM-MLCK). In buffer, the $Ca^{2+}$ $K_d$ values for CaM and CaM-MLCK differ by about two orders of magnitude ($7.2\times10^{-6}$ M and $2.6\times10^{-8}$ M, respectively).[8] Our observation in cells confirms the higher $Ca^{2+}$ affinity of CaM upon binding to MLCK, one of the cellular target proteins. This observation means MLCK can be activated at lower $Ca^{2+}$ concentrations in cells, thereby supporting the idea that target activity may be regulated in cells by differential affinity for CaM at different $Ca^{2+}$ levels.

It has been reported that some proteins adopt a more compact structure in crowded conditions that mimic the intracellular environment.[4e,9] To address whether the structure of Ca-CaM-MLCK in living cells is the same as it is in buffer, we used pseudocontact shifts (PCSs) to derive structural information about Ca-CaM-MLCK in *Xenopus* oocytes. In buffer, PCSs are a well-established tool for obtaining long-range structural constraints.[10] PCSs provide information about the distance and orientation between an observed nucleus and a paramagnetic center. The CaM variant N60D has higher affinity for lanthanide ions at the second $Ca^{2+}$ binding site, so we used the paramagnetic lanthanide ion $Tb^{3+}$ to induce PCSs, which were measured by calculating the difference in the shift between the paramagnetic N60D $(CaTb)_N(Ca_2)_C$CaM and the diamagnetic N60D $(Ca_2)_N(Ca_2)_C$CaM.[11] We used the 3FY-labeled N60D variant to obtain $^{19}F$ PCSs because the $^{15}N$-$^{1}H$ HSQC spectrum of Ca-CaM-MLCK is poorly resolved in oocytes (see Figure S5 in the Supporting Information). As shown in Figure 2 A,B, the $^{19}F$ NMR spectra of the 3FY-labeled wild-type and N60D variant are the same, which suggests that the mutation has a minimal structural effect. Two more resonances appear in the presence of 0.7 equivalents of $Tb^{3+}$, and the population of this species, $(CaTb)_N(Ca2)_C$CaM, is approximately equal to the population of $(Ca2)_N(Ca2)_C$CaM. We calculated a PCS of 0.32 ppm for Y138, and 0.13 ppm for Y99 (Figure 2 C). Inspection of the crystal structure reveals that the labeled position in Y138 is much closer (29 Å) to the $Tb^{3+}$ ion than is Y99 (40 Å). Thus, the PCS for Y138 should be larger than that for Y99, consistent with our observation. When additional $Tb^{3+}$ ions were added (Figure 2 D), the concentration of $(CaTb)_N(Ca2)_C$CaM increased, thus confirming the assignment of the diamagnetic and paramagnetic forms. We then injected $(CaTb)_N(Ca2)_C$CaM-MLCK into oocytes and observed a PCS almost equal to that observed in buffer (Figure 2 E,F). As a consequence of the limited

  

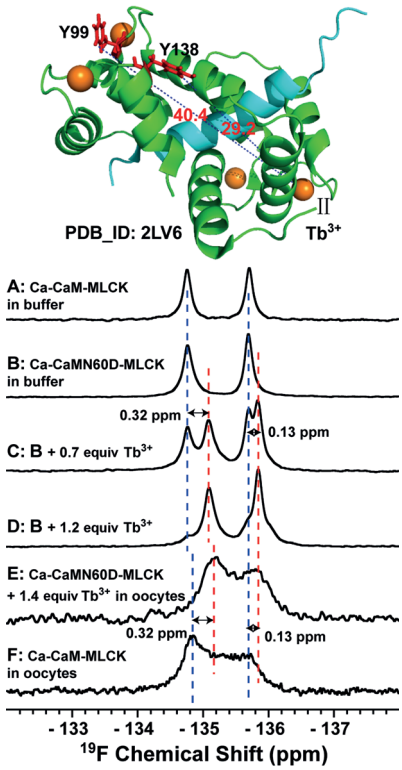


***Figure 2.*** One-dimensional $^{19}F$ NMR spectra of Ca-CaM-MLCK (A), Ca-CaMN60D-MLCK (B), and Ca-CaMN60D-MLCK in the presence of 0.7 equiv of $Tb^{3+}$ (C), 1.2 equiv of $Tb^{3+}$ (D) in buffer, or in the presence of 1.4 equiv of $Tb^{3+}$ in *Xenopus* oocytes (E, a molar ratio of $Ca^{2+}$ to CaMN60D-MLCK of 5:1), and diamagnetic Ca-CaM-MLCK in oocytes (F). The Ca-CaMN60D-MLCK model is shown at the top (PDB_ID: 2LV6). The distances between the $^{19}F$ nuclei and the paramagnetic center (II, $Tb^{3+}$) are indicated.

number of PCS values obtained here, it is difficult to draw a conclusion about cellular effects on the whole protein structure. Nevertheless, our $^{19}F$ PCS data show that it should be possible to obtain long-range structural constraints by including more $^{19}F$ labeling sites.

In summary, we have, for the first time, directly observed the CaM conformational transition in intact *Xenopus* oocytes by using $^{19}F$ NMR spectroscopy. Under physiological conditions, most CaM is in the apo from, and Ca-CaM only appears at high $Ca^{2+}$ levels. The affinity of $Ca^{2+}$ for CaM is enhanced by MLCK in cells, which suggests that MLCK can be actived at lower $Ca^{2+}$ concentration, thereby resulting in further signal transduction. Our observations support the idea that activation of the signaling pathway is regulated by the relative binding affinity of CaM targets at different $Ca^{2+}$ concentrations. Our data also show that in-cell $^{19}F$ PCSs can yield long-range structural constraints. We believe the $^{19}F$ method demonstrated here with CaM can be applied to other cellular signal transduction systems in living cells.

**Keywords:** calmodulin · fluorine · NMR spectroscopy · protein conformation · signal transduction

**How to cite:** *Angew. Chem. Int. Ed.* **2015**, *54*, 5328–5330
*Angew. Chem.* **2015**, *127*, 5418–5420

[1] a) D. Chin, A. R. Means, *Trends Cell Biol.* **2000**, *10*, 322–328; b) K. E. Kamm, J. T. Stull, *J. Biol. Chem.* **2001**, *276*, 4527–4530; c) N. Gao, J. Huang, W. He, M. Zhu, K. E. Kamm, J. T. Stull, *J. Biol. Chem.* **2013**, *288*, 7596–7605.
[2] A. Persechini, B. Cronk, *J. Biol. Chem.* **1999**, *274*, 6827–6830.
[3] a) S. Y. Rhieu, A. A. Urbas, D. W. Bearden, J. P. Marino, K. A. Lippa, V. Reipa, *Angew. Chem. Int. Ed.* **2014**, *53*, 447–450; *Angew. Chem.* **2014**, *126*, 457–460; b) E. Luchinat, L. Barbieri, J. T. Rubino, T. Kozyreva, F. Cantini, L. Banci, *Nat. Commun.* **2014**, *5*, 5502; c) P. Selenko, D. P. Frueh, S. J. Elsaesser, W. Haas, S. P. Gygi, G. Wagner, *Nat. Struct. Mol. Biol.* **2008**, *15*, 321–329; d) D. S. Hembram, T. Haremaki, J. Hamatsu, J. Inoue, H. Kamoshida, T. Ikeya, M. Mishima, T. Mikawa, N. Hayashi, M. Shirakawa, Y. Ito, *Biochem. Biophys. Res. Commun.* **2013**, *438*, 653–659; e) J. A. Hubbard, L. K. MacLachlan, G. W. King, J. J. Jones, A. P. Fosberry, *Mol. Microbiol.* **2003**, *49*, 1191–1200.
[4] a) T. Sakai, H. Tochio, T. Tenno, Y. Ito, T. Kokubo, H. Hiroaki, M. Shirakawa, *J. Biomol. NMR* **2006**, *36*, 179–188; b) Y. Ye, X. Liu, Z. Zhang, Q. Wu, B. Jiang, L. Jiang, X. Zhang, M. Liu, G. J. Pielak, C. Li, *Chem. Eur. J.* **2013**, *19*, 12705–12710; c) Q. Wang, A. Zhuravleva, L. M. Gierasch, *Biochemistry* **2011**, *50*, 9225–9236; d) Z. Serber, R. Ledwidge, S. M. Miller, V. Dötsch, *J. Am. Chem. Soc.* **2001**, *123*, 8895–8901; e) Q. Wang, K. C. Liang, A. Czader, M. N. Waxham, M. S. Cheung, *PLoS Comput. Biol.* **2011**, *7*, e1002114; f) C. Kyne, B. Ruhle, V. W. Gautier, P. B. Crowley, *Protein Sci.* **2015**, *24*, 310–318; g) P. B. Crowley, E. Chow, T. Papkovskaia, *ChemBioChem* **2011**, *12*, 1043–1048.
[5] G. Xu, Y. Ye, X. Liu, S. Cao, Q. Wu, K. Cheng, M. Liu, G. J. Pielak, C. Li, *Biochemistry* **2014**, *53*, 1971–1981.
[6] a) J. L. Kitevski-LeBlanc, F. Evanics, R. S. Prosser, *J. Biomol. NMR* **2009**, *45*, 255–264; b) J. L. Kitevski-LeBlanc, M. S. Al-Abdul-Wahid, R. S. Prosser, *J. Am. Chem. Soc.* **2009**, *131*, 2054–2055.
[7] D. E. Clapham, *Cell* **2007**, *131*, 1047–1058.
[8] T. Porumb, P. Yau, T. S. Harvey, M. Ikura, *Protein Eng.* **1994**, *7*, 109–115.
[9] a) A. Dhar, A. Samiotakis, S. Ebbinghaus, L. Nienhaus, D. Homouz, M. Gruebele, M. S. Cheung, *Proc. Natl. Acad. Sci. USA* **2010**, *107*, 17586–17591; b) B. Akabayov, S. R. Akabayov, S. J. Lee, G. Wagner, C. C. Richardson, *Nat. Commun.* **2013**, *4*, 1615; c) D. Homouz, H. Sanabria, M. N. Waxham, M. S. Cheung, *J. Mol. Biol.* **2009**, *391*, 933–943.
[10] G. Pintacuda, M. John, X. C. Su, G. Otting, *Acc. Chem. Res.* **2007**, *40*, 206–212.
[11] a) I. Bertini, I. Gelis, N. Katsaros, C. Luchinat, A. Provenzani, *Biochemistry* **2003**, *42*, 8011–8021; b) I. Bertini, C. Del Bianco, I. Gelis, N. Katsaros, C. Luchinat, G. Parigi, M. Peana, A. Provenzani, M. A. Zoroddu, *Proc. Natl. Acad. Sci. USA* **2004**, *101*, 6841–6846.

Received: January 12, 2015
Published online: March 5, 2015